Supplementary Information

Supplementary Text:

HRF estimation

Detailed Methods

The hemodynamic response function (HRF) based modeling of the neurovascular coupling is defined as–

$$y(t) = n(t) * h(t)$$

Here, $y(t)$ is used to represent the vascular signal. In an ideal case, the $y\_estimated(t)$ from the convolution product will be same as $y\_recorded(t)$ which is the local vascular concentration changes recorded by NIRS[1]. The HRF is given by $h(t)$ which takes a fixed canonical shape, usually defined by a non-linear gamma variate function, $n(t)$ represents the neural input.

In our work, we processed EEG and NIRS time traces (Materials and Methods, "*Neural and Hemodynamic Signal Processing* ") and then found continuous epochs of ~3.5 minutes, corresponding to 15 blocks of stimulus presentation. These epochs were selected from the entire dataset where transient changes in CPP were within ±5 mmHg. Both the EEG and NIRS (ΔHbO) epochs were mean subtracted to remove any trends in the time-traces and center changes around zero. Finally, $y\_recorded(t)$ was the ΔHbO time-trace and $n(t)$ was the square of the EEG amplitude. The HRF was defined as a six-variable gamma function given by-

$$h(t) = x_1 \times (t)^{x_2} e^{-(t)x_3} - x_4 \times (t)^{x_5} e^{-(t)x_6}$$

Here, t denotes the time and variables $x_1, \dots, x_6$ denote the different shape parameters of the HRF, estimated using a fitting function. For our model, the following constraints were applied on the parameters-

Parameter	Limits	Constraints
x_1	(0,1)	$x_1 > x_4$
x_2	(0,5)	$x_2 > x_3$
x_3	(0,5)	-
x_4	(0,1)	-
x_5	(0,5)	$x_5 > x_6$
x_6	(0,5)	$x_6 > x_3$

A cost-function was defined as the Pearson's correlation (r) between the $y\_recorded(t)$ (from NIRS) and the $y\_estimated(t)$ (from $n(t) * h(t)$).

Random sampling was used to select 10,000 uniformly distributed random numbers within the bounds of the six-variable space corresponding to $x_1, \dots, x_6$ and $h(t)$ evaluated for all the 10,000 values. The cost-function was then calculated between the $y\_estimated(t)$ and $y\_recorded(t)$ signals for all the 10,000 $h(t)$. The best 5% (500 initial selections for $x_1, \dots, x_6$ with highest r) were selected as initialization points for the fitting algorithm. A gradient-descent based search algorithm[2] was used to find best-fit values for $x_1, \dots, x_6$ with the aforementioned constraints and limits which minimizes the cost-function (- r). This gave a single $h(t)$ corresponding to the best estimation of HRF for that data epoch. This process was repeated for multiple epochs at different CPP values across all three subjects. A potential caveat of selecting Pearson's r as our cost-function is that it is insensitive to amplitude differences between the recorded and the estimated hemodynamic signals. This was primarily done to ensure the HRFs were not biased by SNR based magnitude variations in EEG or NIRS signals. Hence, for all our subsequent analyses, we normalized our HRFs (by z-score) and only focused on changes in shape of the HRF.

Robustness of the solution was checked by cross-validating fits against a "noise distribution". For each subject, 15 epochs of resting state hemodynamic signals (ΔHbO using NIRS) were identified with similar timescales (~3.5 minutes) as the evoked ΔHbO data. Resting state was identified as a period of recording where no stimulus was presented. These were either periods before starting the stimulus protocol or rest data recorded at the beginning of the experiment. The resting state hemodynamic signals were also filtered and processed the same way as evoked NIRS signals. This collection of epochs of resting state ΔHbO was treated as resembling physiological "noise" in the context of evaluating evoked neurovascular coupling. Finally, every evoked EEG epoch was used to evaluate a best-fit HRF against all the 15 resting state hemodynamic signals. This created a distribution of r values corresponding to "fits to unrelated signal or noise". Only HRFs from evoked data, with corresponding best-fit r above the 75th percentile of the aforementioned distribution, were included for further analysis and trends. Additionally, we also checked for the validity of the solution by varying the number of initialization points (500 ± 100). The solution was found to be stable and consistent across all different number of initial selections. Finally, this resulted in n=26 HRFs estimated at different CPPs between 40-120 mmHg, which were used for further analysis.

Discussion:

The most commonly used form of $n(t)$ is a binary sequence showing 1 at stimulus onset (or for the duration it is present on screen) and 0 indicating stimulus off.[3,4] This use of a proxy-neural signal has been called to question by previous studies, arguing that the neural signal may alter with adaptation during long stimulus durations[5] or pathophysiology[6] which can alter neurovascular coupling. Previous literature that has tried to understand the neural origins of vascular BOLD signals, have found that the power of the local field potential most closely resemble the cellular metabolism which is assumed to be the reason for functional hyperemia[7–9]. Hence, in our analysis, we use broadband power (0.5-30 Hz) of the recorded EEG signals to estimate the hemodynamic signals. A potential limitation, however, of using a physiological neural signal is the presence of noise in the estimate. Hence, to clearly distinguish fits to evoked responses against those to noise, we tested against a physiological 'noise' signal, specifically, resting-state hemodynamics. 75th percentile (of the r_{fit_noise}) was selected as the threshold distinguishing between good and bad fits. This was chosen to set a relatively low threshold for fit quality, through which we were able to retain a large number of data sets for further analysis. Significance testing was performed at a later stage, in subsequent analyses with HRFs (Figure 4c, Supplementary Figure 3).

Supplementary References-

1. Huppert TJ, Hoge RD, Diamond SG, et al. A temporal comparison of BOLD, ASL, and NIRS hemodynamic responses to motor stimuli in adult humans. *Neuroimage* 2006; 29: 368–382.
2. Byrd RH, Hribar ME, Nocedal J. An Interior Point Algorithm for Large-Scale Nonlinear Programming. *http://dx.doi.org/101137/S1052623497325107* 2006; 9: 877–900.
3. Lindquist MA, Meng Loh J, Atlas LY, et al. Modeling the hemodynamic response function in fMRI: Efficiency, bias and mis-modeling. *Neuroimage* 2009; 45: S187–S198.
4. Aarabi A, Osharina V, Wallois F. Effect of confounding variables on hemodynamic response function estimation using averaging and deconvolution analysis: An event-related NIRS study. *Neuroimage* 2017; 155: 25–49.
5. Buxton RB, Uludağ K, Dubowitz DJ, et al. Modeling the hemodynamic response to brain activation. *Neuroimage* 2004; 23: S220–S233.

6. Lindauer U. Pathophysiological interference with neurovascular coupling - when imaging based on hemoglobin might go blind. *Front Neuroenergetics* 2010; 2: 25.
7. Logothetis NK, Pauls J, Augath M, et al. Neurophysiological investigation of the basis of the fMRI signal. *Nature* 2001; 412: 150–157.
8. Logothetis NK. The neural basis of the blood-oxygen-level-dependent functional magnetic resonance imaging signal Nikos. *Philos Trans R Soc Lond B Biol Sci* 2002; 357: 1003–37.
9. Liu Z, He B. fMRI–EEG integrated cortical source imaging by use of time-variant spatial constraints. *Neuroimage* 2008; 39: 1198–1214.

Supplementary Figures:

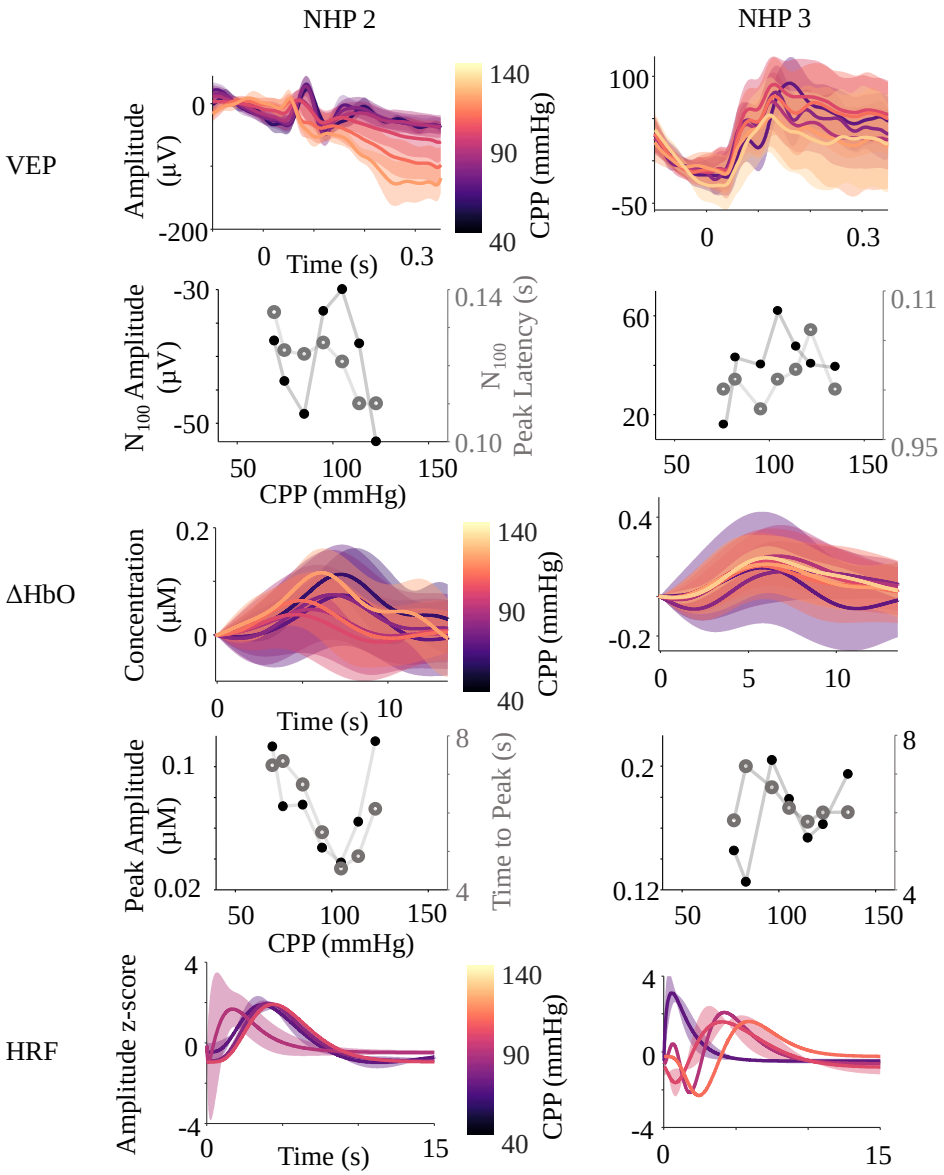

Supplementary Figure 1. Trends in evoked neural (VEP), hemodynamic (ΔHbO), and neurovascular coupling (HRF) signal with CPP for NHP 2 and 3 (similar results for NHP 1 are shown in Figure 2 and 4a). The plots show the mean (bold line) and s.d. (shaded region) for VEP, ΔHbO, and the HRF calculated in bins of 10 mmHg from 40-140 mmHg CPP. The HRF was evaluated by convolving epochs of ~3.5 minutes of simultaneous EEG and NIRS signal at different CPP levels (see Supplementary Text and Materials and

Methods). The color bar for all VEP, ΔHbO and HRF line plots are indicated on respective plots for NHP2 going from black (40 mmHg) to light yellow (140 mmHg). NHP3 plots follow the same color scheme.

Each evoked response shows a variation with CPP which is further quantified by plotting the VEP N_{100} and ΔHbO peak feature changes with CPP (latency (gray open circles) and amplitude (black filled circles)). These specific features change with CPP; however, they do not fully capture the variation in the evoked neural and vascular waveforms. Additionally, while changes with CPP in the VEP and ΔHbO is seen in all the subjects, the inter-subject variability makes comparison hard. The stimulus-evoked neural and vascular signals are thus used to estimate the neurovascular coupling, through a semi-constrained HRF model. The HRFs also show changes with CPP, with the consistent presence of an “initial dip” at extreme values, potentially caused by cerebral autoregulatory failure.

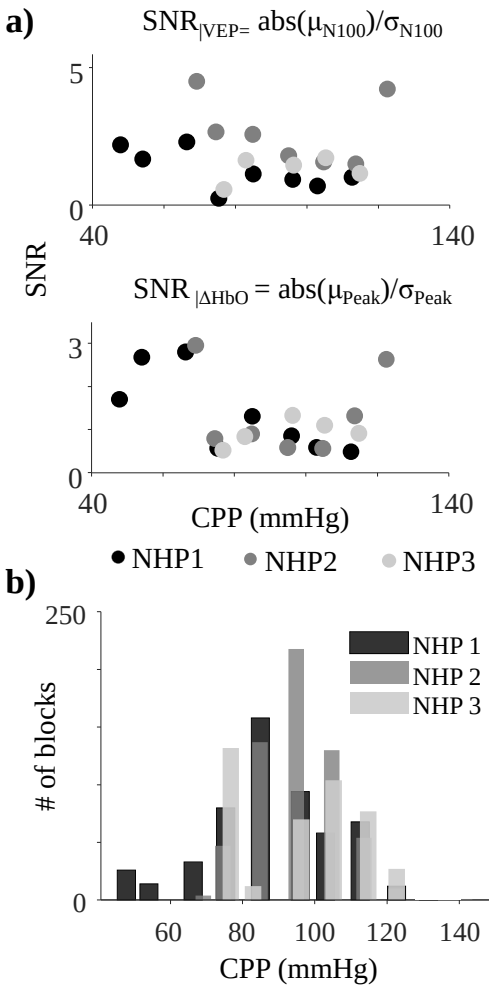

Supplementary Figure 2: Changes in signal-to-noise ratio as a function of CPP. a) SNR was calculated for all subjects as the ratio of mean (μ) to the s.d. (σ) at N_{100} for the evoked neural responses, and the peak concentration change for ΔHbO for the evoked hemodynamic responses. Across all three subjects, no significant trend was found in the SNR for VEPs ($p\text{-value}_{NHP1} = 0.7435$, $p\text{-value}_{NHP2} = 0.3024$, $p\text{-value}_{NHP3} = 0.7825$) or ΔHbO ($p\text{-value}_{NHP1} = 0.5517$, $p\text{-value}_{NHP2} = 0.9063$, $p\text{-value}_{NHP3} = 0.1095$) responses across different CPPs. b) Some of the observed variations in SNR at high and low CPP can be explained by the differences in samples across different CPP. These are indicated in the bar plot over a range of 40-140 mmHg.

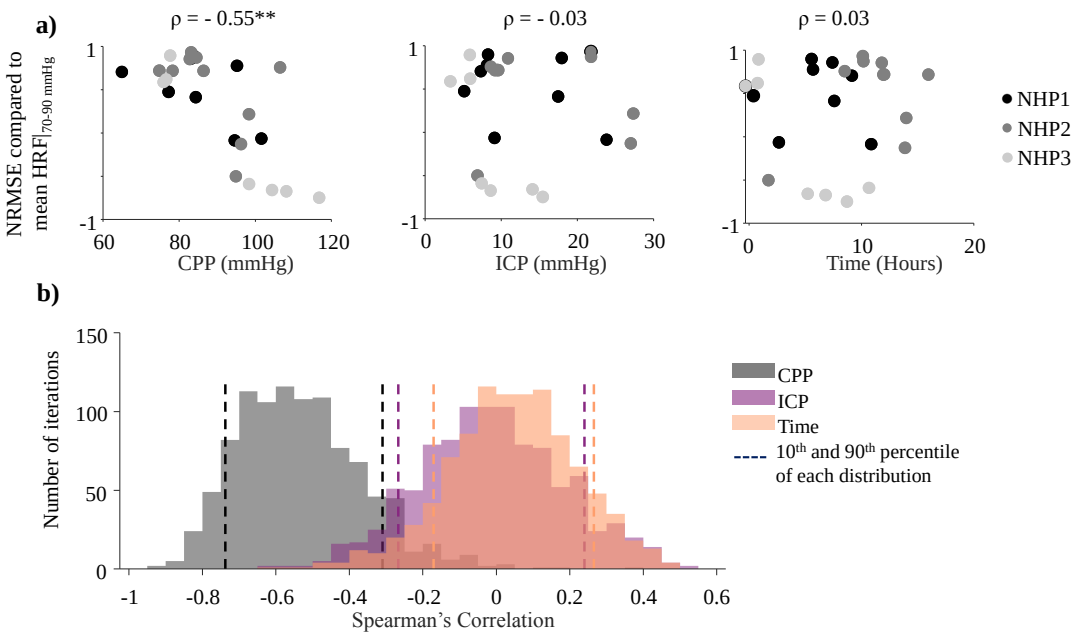

Supplementary Figure 3. The HRF shape variations (neurovascular coupling changes) as a function of CPP, ICP, and time. ICP was altered in our experiments to change CPP and hence, could influence HRF changes. Changes with time were tested to check for effects of duration under anesthesia on neurovascular coupling. NRMSE was calculated between a baseline healthy HRF for that subject (mean HRF between 70-90 mmHg), and every HRF estimated at different CPP levels. This was then plotted against the recorded CPP, ICP or time reported during the epoch of signals used for the respective HRF estimation.

(a) Changes in HRF were most significant with CPP (ρ_{CPP}=-0.55, p-value$_{CPP}$=0.0049) showing a decrease in similarity with the healthy baseline at higher CPP levels, potentially linked to the state of autoregulatory health. However, trends with ICP (ρ_{ICP}=-0.03, p-value$_{ICP}$=0.8845) or time showed no significant correlation (ρ_{time}=0.03, p-value$_{time}$=0.8728).

(b) Further, a bootstrap analysis for the ρ values of each, 1000 times with replacement, showed that trends with CPP were indeed the most prominent amongst all. The 90th percentile of the CPP ρ distribution was greater than the lowest 10th percentile of the time or ICP distribution.

These results affirm the contribution of CPP, specifically autoregulatory health, in changing neurovascular coupling.